

# Toward an Adaptive Foot for Natural Walking

Cristina Piazza<sup>1</sup>, Cosimo Della Santina<sup>1</sup>, Gian Maria Gasparri<sup>1</sup>, Manuel G. Catalano<sup>1,2</sup>,  
Giorgio Grioli<sup>1,2</sup>, Manolo Garabini<sup>1</sup>, Antonio Bicchi<sup>1,2</sup>

**Abstract**—Many walking robot presented in literature stand on rigid flat feet, with a few notable exceptions that embed flexibility in their feet to optimize the energetic cost of walking. This paper proposes a novel adaptive robot foot design, whose main goal is to ease the task of standing and walking on uneven terrains. After explaining the rationale behind our design approach, we present the design of the SoftFoot, a foot able to comply with uneven terrains and to absorb shocks thanks to its intrinsic adaptivity, while still being able to rigidly support the stance, maintaining a rather extended contact surface, and effectively enlarging the equivalent support polygon. The paper introduces the robot design and prototype and presents preliminary validation and comparison versus a rigid flat foot with comparable footprint and sole.

## I. INTRODUCTION

Humanoid robots are very complex systems, whose design, implementation, control and operation are in general tougher problems, especially when compared to traditional robots. Locomotion and manipulation are probably the two most complex actions of a humanoid robot, that attract the attention of the research community. Successfully walking in a complex non-structured environment is still at the edge of the state of the art of robotics [5]. Interestingly, while much attention in manipulation is devoted to hand design very little research has been conducted so far in foot design for locomotion. It is opinion of the authors that one of the key elements that could determine substantial improvement in the field of walking robots is the foot design. The wide majority of humanoid robots existing in literature adopt flat feet. Valuable exemplars include: ATLAS [5], HUBO [23], HRP3 [17], Nao [11], Walkman [22]. However some examples of different architectures exist, such as actuated feet which actively partially adapts to the environment [10][18][19], and flat feet with compliant elements [20][21][29]. So far, biomimetic adaptive feet that try to mime the human foot adaptability and elasticity were only theorized in [28]. More effort was devoted in the design and application of ankle-foot prostheses, since, on the one hand, a human operator is able to fully exploit the intrinsic prosthesis potential; on the other hand, issues such as decreasing metabolic cost are fundamental for a comfortable day use [12][14][6]. However the application of such systems in robotics is not so common (see e.g. [7]). One of the main reason of the scarce use of

This work is supported by EU Project WALKMAN and ERC Advanced Grant SoftHand

<sup>1</sup>Research Center “Enrico Piaggio”, University of Pisa, Largo Lucio Lazzarino 1, 56126 Pisa, Italy

<sup>2</sup>Department of Advanced Robotics, Istituto Italiano di Tecnologia, via Morego, 30, 16163 Genova, Italy

cristina.piazza@ing.unipi.it



Fig. 1. SoftFoot performing a push-off phase.

such systems, is that they are not typically compatible with flat floor hypothesis [30]. In other words, they complicate the locomotion instead of simplifying it. In the last decades much effort was devoted to the design of new robotic systems embedding functional principles into their mechanics. Through this *embodied intelligence* approach, the system should be able to cope with part of the problem complexity directly at a mechanical level, resulting in a simplification of planning and control. Among the main ingredients of such research approach are under-actuation [4], introduction of compliant element in the mechanics [1], and a human-aware look to the system design [2]. One field that largely took advantages of these drivers is the design of robotic hands, see e.g. [9].

In this work we propose to use a similar approach for the development of new robotic feet. We first explore the main guidelines toward the design of a foot which could manage uneven terrain interactions through its intrinsic adaptivity. Starting from these considerations a first prototype is proposed, called SoftFoot (see Fig. 1). The SoftFoot is a completely passive system, which varies its shape and stiffness in function of the exerted forces, through a system of pulley, tendons and springs opportunely placed in the structure. The paper is organized as follow: in section II we introduce some basic concepts justifying the use of adaptive feet in locomotion, in section III the foot design is discussed and the SoftFoot prototype is presented, and in section IV experimental results are provided showing the effectiveness of the proposed system in achieving the goals.

## II. PROBLEM DEFINITION

### A. Theoretical Background

Consider a humanoid robot in the single-support phase, supported by its foot laying on the ground. The combined

effect of gravity, body dynamics, interactions of the upper body with the environment, etc., yield a system of forces acting on the robot, which can be characterized by the total resulting force  $F_A$  acting on the robot and their total momentum with respect to its center of mass  $M_A$ . For the robot to be able to stand in that configuration  $F_A$  and  $M_A$  need to be compensated by the ground-foot interaction.

Assuming that the ground-foot contact is without sliding, static friction compensates for the component of  $F_A$  parallel to the ground, and for the component of  $M_A$  orthogonal to the ground. Assume that the ground compensates for the component of  $F_A$  orthogonal to the ground itself, the components of  $M_A$  tangent to the ground, are the only actions left to compensate. Literature calls Zero Moment Point (ZMP) a point on the ground surface with respect to which such components are null.

Considering the case of flat foot lying on flat ground, the ZMP is always well defined whenever the component of  $F_A$  orthogonal to the ground is greater than zero. It is a well-known result, in literature, that a robot supported by a flat foot in contact with flat ground is balanced if the ZMP is contained in the set of points that establish the contact area. In the case of multiple coplanar flat contacts this result extends to the convex hull of all the contact regions [24]. Several works were devoted to the generalization of ZMP stability test to uneven terrain. Important examples are [26], [27] and [8]. The characterization of force distribution on non planar surfaces, on the other hand, which generalizes the concept of Center of Pressure is treated and generalized in [3].

Taking two general surfaces, we call  $S$  their contact region, i.e. the set of areas and points in which the two surfaces are in contact (see Fig. 2). We call the contact convex hull  $C(S)$  the smallest convex portion of the two surfaces that encloses every contact point and/or area. We will suppose in the following that a plane  $P$  exists such that  $C(S) \subset P$ .

If the bodies are compliant, finite portions of the surface may come into contact, and if friction is present, torques may also be exerted.

It results in a transmission of a distribution of contact tractions over  $S$ . At each point  $r$  of the contact area  $S$ , bodies mutually exert traction. Be  $P(r) = [P_x(r), P_y(r), P_z(r)]^T$  the traction for every point  $r \in S$  expressed in a frame tangent to the contact, such that the component  $P_z$  is that normal to the tangent plane. The  $P_x$  component is usually referred to as pressure, while  $P_y$  and  $P_z$  are the friction components. The tractions are assumed to be compressive, that is,  $P_x(r) \geq 0 \forall r \in S$ . Adhesive forces between bodies are therefore disregarded by this model.

The overall resulting contact force that is exerted by the ground is  $F_c \triangleq \int_S P(r) dr$ .

A contact centroid  $c$  [3] for  $S$  and  $P$  is a point such that a set of forces equivalent to  $P$  exists, having the following characteristics: i) it is comprised of only a force and a torque; ii) the force is applied at that point, and is directed into  $S$ ; iii) the moment is parallel to the surface normal at that point.

*Theorem 1:* Be  $P_x(r) \geq 0 \forall r \in S$ , i.e. the contact pressure

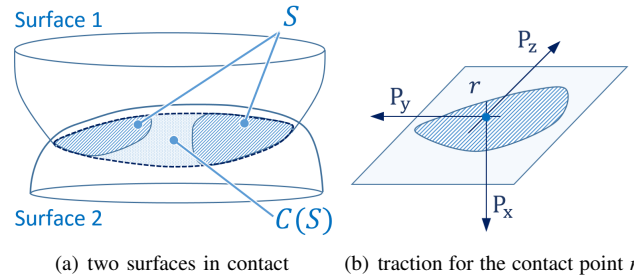


Fig. 2. Two surfaces in contact (a):  $S$  is the eventually non-convex contact area,  $C(S)$  is the convex hull of  $S$ . In (b) we report the traction  $P(r)$  exerted in a generic contact point  $r \in S$ .

can only be directed towards the inside of the bodies. Thus  $c \in C(S)$ , i.e. contact centroid lies in the contact surface convex hull.

By considering the robot foot sole and the ground as the two contacting surfaces, the next corollary derives directly:

*Lemma 1:* If a system of forces acting on a robot admits ZMP  $z$  on a generic ground surface and  $z \in C(S)$ , then a distribution of contact forces exists such that it balances the system of forces, and the robot is in equilibrium.

This generalization of ZMP balancing condition leads to the design guideline that, to improve the robot stability, feet architectures that maximize the convex hull  $C(S)$  should be considered. Given a flat solid ground, it is clear that a flat rigid foot is the best option to obtain this result, on the other hand, in the presence of a generic uneven terrain, different designs can obtain better results.

In the following we discuss and test the use of soft and adaptive designs in order to increase the surface  $S$ , and hence  $C(S)$  on uneven terrain.

### B. Rigid vs Soft foot

For the sake of simplification, we reduce the problem by considering it two-dimensional and static. A robot standing on a flat foot can be modeled as a static table-cart system [16], as that shown in Fig. 3 (a). Referring to the figure, the sole force acting on the robot (excluding the ground) is gravity, thus the ZMP corresponds to the vertical projection of the center of mass (COM) on the ground. It is easy to show that all the set of points, in which the COM can be moved so that the ZMP falls within the contact surface (which is the foot sole), admit a balancing reaction force distribution.

In the case that the foot steps over a small obstacle, as in Fig. 3 (b), two negative effects arise. First, the obstacle induces a rotation  $\alpha$  on the foot, which tends to displace the COM by  $\alpha_H$ . Unless this displacement is very small, it needs to be compensated by a rotation of the ankle of an angle  $\theta - \alpha$ , which we assume. Second, the convex hull of the contact surface shrinks (to the colored segment, which is sensibly shorter of the feet length).

A possible approach to improve the rigid flat foot would be to make a compliant flat foot as in Fig. 3 (c). This foot differs from the rigid flat foot for a layer of soft material between the rigid parts of the foot and the ground. The heuristic behind this choice is that a soft foot could absorb the obstacle, as

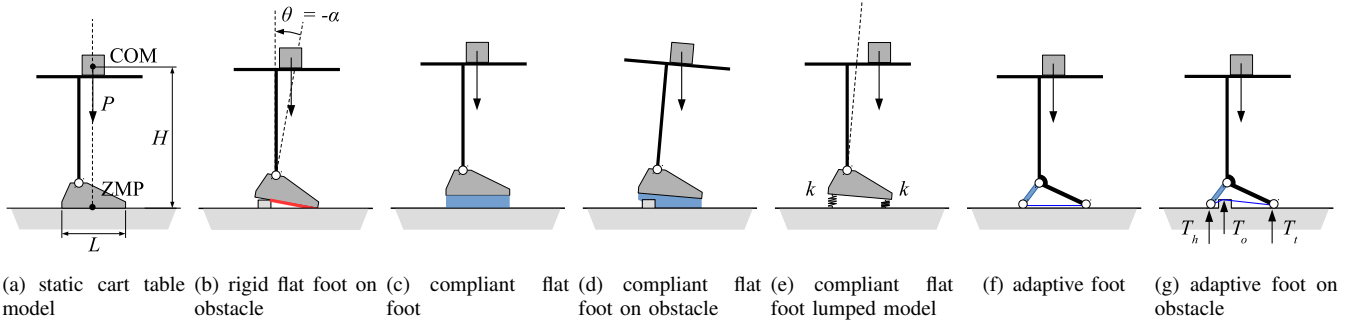


Fig. 3. Static cart table models of different feet described in section II.

in 3 (d), thus avoiding the need for ankle compensation and, moreover, keeping a larger contact surface.

One may think that the softer is the foot sole the better. However lower limits exist for the sole stiffness. To understand why, consider the simplified compliant flat foot model of Fig. 3 (e), where all the compliance is concentrated in two springs supporting the tip and the heel of the foot, standing on a flat ground. Moving the robot COM forward by  $x$  from the vertical line above the foot mid point yields a rotation of the foot of an angle  $\alpha \approx x2P/kL^2$ . Physical limits on the range for the ankle motion  $|\theta| < \theta_{max}$ , yields a lower bound on

$$k > k_{min_s} = P/L\theta_{max},$$

below which the ankle can not compensate for the foot rotation over all the possible contact surface and keep the robot vertical (which means that if  $k < k_{min}$  feasible support length shrinks with respect to the full contact surface). A second practical limit to the sole stiffness comes from the necessity for the system equilibrium to be stable. It is in fact well known that an elastic inverted pendulum is stable on the topmost equilibrium if the torsional stiffness  $k_\theta > mgH$ , that in our simplified model translates as

$$k > k_{min_g} = 2mgL^2/H.$$

If this second condition is not met, it would be in practice impossible to keep the robot standing passively, and equilibrium would require a possibly expensive active control.

A different solution, which constitutes the basic idea of the system we propose in this paper, is that of an adaptive mechanism as that of Fig. 3 (f). This foot is composed of a frontal arch, which connects to the robot through the ankle and lays on the ground on the foot tip, and a backward heel arch, idle on the ankle, which supports the back side of the foot thanks to a flexible traction beam which holds the two arches together. The equilibrium of this foot on a solid flat ground is the same of that of a rigid foot, thus avoiding the tilting problems of compliant flat feet, but lets the foot adapt to obstacles as in the example of Fig. 3(g). Some calculations can be used to show that the contact force balance so as to

obtain<sup>1</sup>:

$$T_h = P \frac{(L - x_{com})}{L} (1 - \tan \alpha_1 \tan \alpha_H) \quad (1)$$

$$T_o = P \frac{(L - x_{com})}{L} (\tan \alpha_1 + \tan \alpha_2) \tan \alpha_H \quad (2)$$

$$T_i = P \frac{(x_{com} - L)(\tan \alpha_2 \tan \alpha_H) + x_{com}}{L}, \quad (3)$$

which are all always positive (thus admissible) as long as the  $x$  coordinate of the COM  $x_{com} < L$  (in analogy with the rigid foot) and

$$x_{com} > L \left( \frac{1 - \tan \alpha_H \tan \alpha_2}{\tan \alpha_H \tan \alpha_2} \right).$$

It is worthwhile noting that although it is adaptive, the foot of Fig. 3(f), displays infinite stiffness once the contact with the ground is acquired. This property which is desirable in terms of stability of the support, performs poorly in terms of step shock absorption, where a compliant flat foot as that of Fig. 3 (c) would probably offer better performance. The solution that is presented in the next section has a non-linear stress-stiffening plantar arch mechanism, as shown in Fig.6 whose precise analytical solution is too long to fit in this paper.

### III. SOFTFOOT

Thanks to a complex system of 26 bones, 20 muscles and more than 100 ligaments, the human foot behaves as a complex but still operative and performing biomechanical structure. It is capable to withstand the weight of the human body, but be flexible and elastic enough to assist the body in a variety of challenging tasks (e.g. running, climbing, balancing). Foot bones are distributed along two main concurrent structures, called arches: the *longitudinal arch* and the *transverse arch* (see e.g. [25]). The *longitudinal arch*, as depicted in Fig. 4 (a), form a triangular geometry composed by the *Calcaneus*, a set of metatarsal bones, *Phalanges* and, on the foot base, a connective tissue, named *Planar Fascia*. This geometric distribution, together with tendons and muscles, creates so-called *Foot Windlass Mechanism*, studied first by Hicks in 1954, see [13]. In engineering (e.g. in yachting) windlass mechanisms are adopted to move heavy

<sup>1</sup>The angles  $\alpha_1$  and  $\alpha_2$  are the angles the traction beam forms with the flat ground on the tip and heel, respectively, while  $\alpha_H$  is the angle that the backward heel arch forms with respect to the vertical direction.

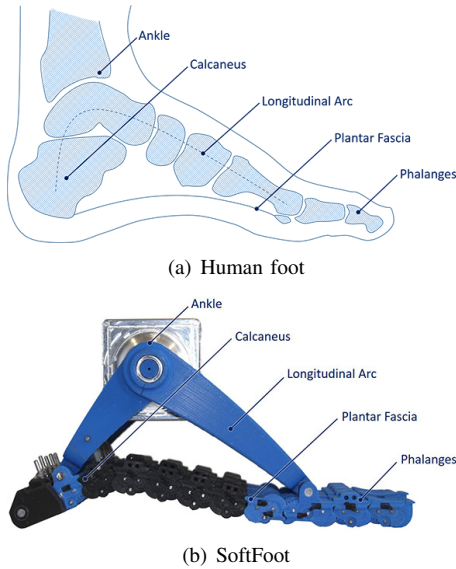


Fig. 4. Architecture of the Human foot, bones, phalanges and representation of the *longitudinal arch*, (a). Prototype of the SoftFoot, with highlighted components adopted for the implementation of the artificial *longitudinal arch*, (b).

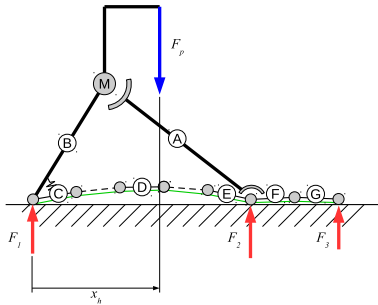


Fig. 5. Architecture of the SoftFoot, simplified kinematic with the main parts underlined.  $F_1, F_2, F_3$  are the three considered contact forces,  $F_p$  is the load applied by the robot, which is connected to body (B) through the ankle. (F-G) represent the phalanges. The plantar fascia is implemented by the set of links (C-D-E) and the tendon (green in figure) which is connected from the calcaneus to the tip of the toe. The bodies (C-D-E-F-G) are connected each other through a spring of stiffness  $e$ . Bodies (B-C) are also connected through a spring of stiffness  $e_0$ .

loads, in foot mechanics the windlass mechanism describes the tightening action of the long plantar fascia of the foot to maintain arch stability when the heel come off the ground (late stance phase of the gait). This special architecture is responsible for many of the main features of the foot system: energy storage - when the phalanges turns up the plantar fascia is pulled - impacts absorption - if an impulsive load is applied on the plantar fascia the longitudinal arch elastically flex - adaptiveness - the plantar fascia is soft and can absorb irregularities of the terrain - and stabilization - when the body weight acts on the ankle the foot becomes more rigid and stable.

The foot prototype presented in this paper aims to transfer in a robotic system some of these peculiarities, implementing a mechanical architecture that translates in a feasible

engineered complexity the behavior of a human foot. Fig. 4 (b) shows the proposed prototype. All the components are realized through rapid prototyping techniques. Fig. 5 shows its simplified kinematic, while Fig. 6 shows simulation results which drove the design of the SoftFoot prototype. As in the human example, the proposed system presents a stiffening-by-compression behavior, being compliant when the load is low (i.e. when the contact occurs) and rigid when the load grow, correctly supporting the weight of the robot (Fig. 6 (d)). Fig. 6 (a-b) shows how the foot compliance can be chosen by changing the calcaneus and plantar fascia stiffnesses (Fig. 5). Fig. 7 shows in detail the parts which implement the SoftFoot. The three-dimensional view of Fig. 7 (a) shows as the SoftFoot is made of simple, compact and modular mechanical structures. The function of the longitudinal arch is recreated through components (2) and (3). These components are connected one to the other with a revolute joint. Component (2) is rigidly linked to the output shaft of the actuator (1), which represents the ankle joint. The foot sole is realized by five modular, elastic and flexible structures (6,7,8,9,10) connected with revolute joints (e.g. components 6A and 6D) to parts (2) and (3). As it was also proposed in [28], the feet structure is split in 5 parallel sagittal mechanisms to facilitate adaptation of the feet to irregularities of the ground surface in the lateral direction. A detailed analysis of the lateral deformation dynamics of the SoftFoot is too wide to fit in this paper and is demanded to future extensions. Each flexible mechanism (6,7,8,9,10) is realized by a series of rolling joints. The design of these joints, similar to those used in the Pisa/IIT SoftHand [9], are an evolution of Hillberry's joint [15], designed to be very robust and easy to combine. Each module is connected to another by a pair of elastic bands (green in Fig. 7 (c)) and a tendon (red in Fig. 7 (c)). The tendon follows a specific route along the flexible structure to allow proper force distribution, implementing a mechanical counterpart of the *Plantar Fascia* between components (6D and 6A). On the back side of the robotic foot the five flexible structures are held together by an additional part (4). The group of parts (4, 6A, 7A, 8A, 9A, 10A, and 2) resemble the *Calcaneus* of a human foot. On the front side of the foot, connected parts (6B and 6E, 7B and 7E, 8B and 8E, 9B and 9E, 10B and 10E) represents the phalanges of a human foot. In order to provide elasticity and to avoid singularities, along the longitudinal axis five springs (5) are placed, each spring making an elastic connection between part (2) and each flexible mechanism (6-10). SoftFoot mechanical structure can be easily extended to include tendons routed through the feet to simulate muscle action, but the study of their effect is demanded to future work.

#### IV. EXPERIMENTAL RESULTS

In this section we present experimental results showing the effectiveness of the proposed design in improving robot stability and adaptation capabilities on uneven terrains (both in artificial and real environment). To make a clear and fair analysis, for each experiment a comparison with an

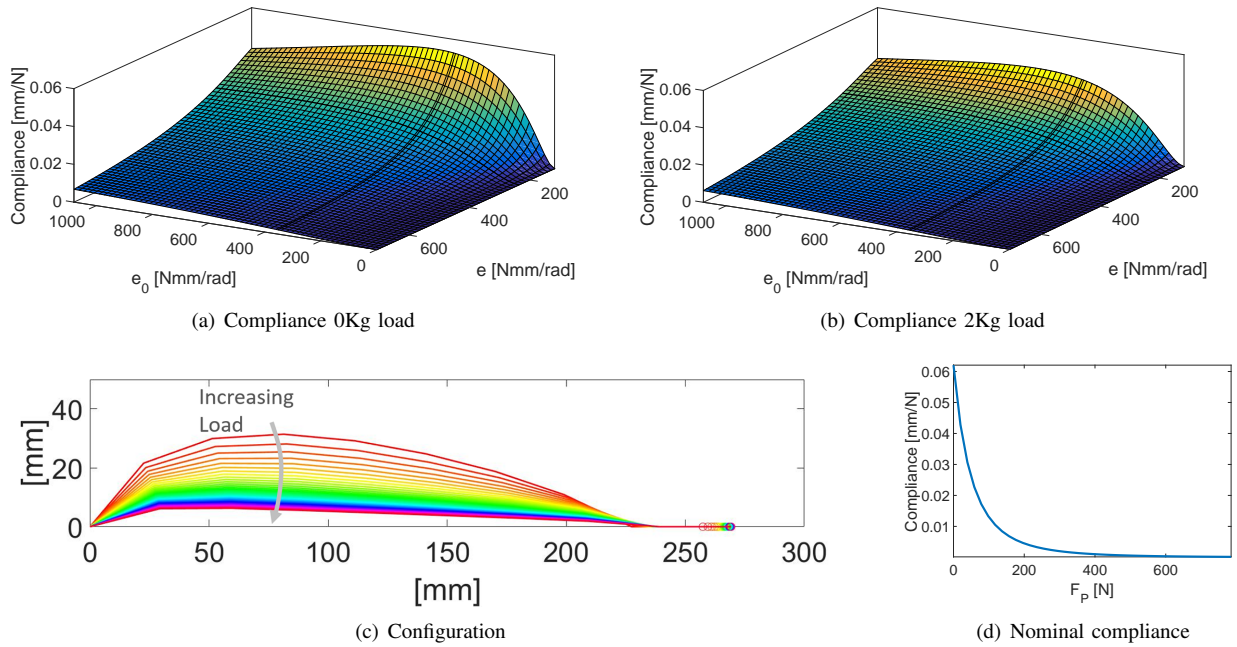


Fig. 6. Simulative results supporting the design of the foot. (a-b) show foot compliance with respect to the load, for various values of plantar fascia stiffness  $e$  and calcaneus stiffness  $e_0$ . The nominal stiffness implemented in the prototype are evidenced in black. For the nominal values, (c) shows the configuration of the links of the plantar fascia and phalanges for a load which varies from 0Kg to 80Kg. Panel (d) displays the vertical component of the foot compliance with respect to the same loading conditions of panel (c). The SoftFoot presents a stiffening behavior, soft for low loads when the contact occurs, and rigid for large loads when it has to support the robot. For the sake of space, we will report the derivation of the simulative model in future extensions of the work.

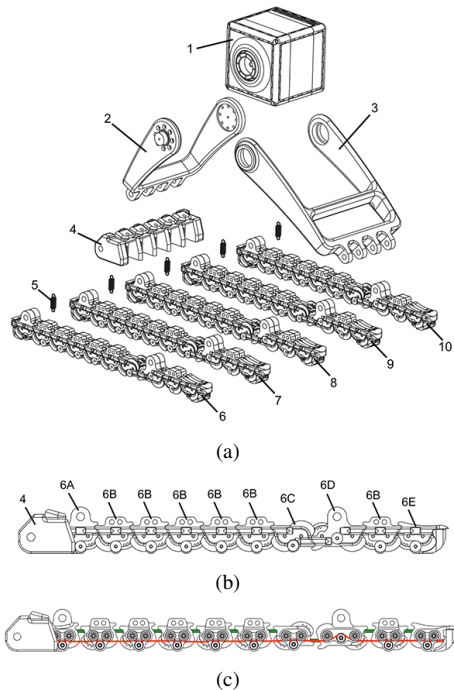


Fig. 7. Exploded view of 3D CAD model of the SoftFoot prototype (a). Lateral view, (b), and exploded lateral view, (c) of flexible structures (ie. 6) which forms the sole of the SoftFoot. In (c) the elastic bands are highlighted in green, while the cable routing is red.

equivalent rigid foot with same size and weight (see 8 (a), part (3)) has been performed. As previously discussed the

simple rigid foot design is the most widely used in robotic, since it allows to obtain the largest supporting area in the flat terrain case.

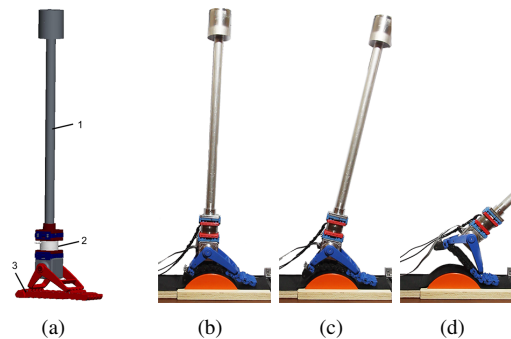


Fig. 8. Picture (a) show a schema of the experimental setup adopted for the evaluation of the support polygon of each foot. Component (3) represent a 3D view of the rigid foot used. Fig. (b,c,d) show a sequence of an experiment performed with the SoftFoot on a round obstacle.

Fig. 8 (a) shows the experimental setup. A rigid bar (1), with a fixed mass on the top, is mounted on top of the ankle joint. A Force/Torque (2) sensor (ATI Mini45) is placed between the two parts. The total weight on top of the sensor is 15N. The center of gravity is fixed at 250mm from the ankle axis. The first column of Table I shows dimensions and shapes of the eight different terrains adopted in the experimental sessions. The overall system behaves as an inverse pendulum, the motor of the ankle has been controlled in order to move the beam in forward

and backward directions. For each terrain each foot has been placed on a predefined position. If a foot was not able to stand on the obstacle it was moved to the nearest stable positions. The stability region was then evaluated by moving the pendulum forward and backward until it falls. The pendulum movement was very slow, i.e.  $0.1 \frac{\text{deg}}{\text{s}}$ , in order to avoid dynamic effects. Fig. 8 (b,c,d) show a sequence of the evolution of an experiment where the SoftFoot is tested on a round obstacle. To measure the extension of the support polygon readings of the F/T sensors and of the ankle joint encoder were combined to project the forces on vertical and frontal directions of the sagittal plane, obtaining  $F_x$  and  $F_z$ , respectively and then using the definition of CoP with respect to the underlying flat base. Table I reports the results of the experimental sessions. The SoftFoot design is compared to the rigid flat foot in terms of linear extension of the support polygon (Support length) and compensatory ankle pitch angle to keep the leg vertical (Ankle pitch). Pictures of the starting condition of the experiments and the behavior of the adaptation capabilities of the feet are also included in each cell. The SoftFoot shows a smaller compensatory ankle pitch angle than the rigid foot on the more uneven terrains, and equal results in the two flat grounds. Furthermore, it is worth to note that in the cases of experiments with the SoftFoot, the support polygon is wider than the one obtained with the rigid foot for six over eight terrains. Note that the shorter support length with respect to the rigid foot in the flat case is due to the presence of the toe articulation in the SoftFoot. It is reasonable to think that such improvements would increase the region on which the robot could exert forces and decrease the tilting momenta, and thus reduce the control effort needed to balance the robot in case of locomotion on uneven terrain. Finally Fig. 9 shows some pictures of the SoftFoot and its passive adaptive capabilities on real-world uneven terrains.

## V. CONCLUSIONS AND FUTURE WORKS

This paper introduced a novel compliant robot foot design, whose main goal is to ease the task of standing and walking in realistic uneven terrains. After briefly recalling the theory of standing and walking robots, which motivates our work, the idea behind the presented foot was introduced, highlighting the differences with respect to the most common foot design adopted in literature. The presented foot adapts to uneven terrains while still being able to rigidly support the standing feet and to maintain a good extension of the contact surface, effectively extending the equivalent support polygon. Preliminary experimental validation and comparison to rigid flat foot design were reported. Both the design and the validation experiment presented in this paper show just preliminary results which the authors aim to improve in their future works. In particular, future investigation will deal with the optimization and the characterization of the windlass mechanism to improve the push-off movement, and characterize and extend the SoftFoot adaptation capabilities also to terrain profile variations along the direction of the frontal plane.

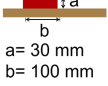
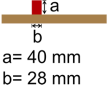
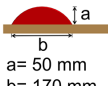
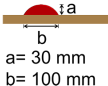
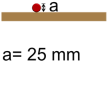
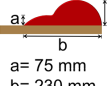
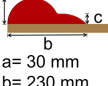
		
	 219 mm $0^\circ$	 134 mm $0^\circ$
 a = 30 mm b = 100 mm	 67 mm $3^\circ$	 94 mm $4^\circ$
 a = 40 mm b = 28 mm	 40 mm $-26^\circ$	 79 mm $23^\circ$
 a = 50 mm b = 170 mm	 17 mm $25^\circ$	 53 mm $10^\circ$
 a = 30 mm b = 100 mm	 61 mm $-22^\circ$	 112 mm $13^\circ$
 a = 25 mm	 46 mm $-11^\circ$	 78 mm $17^\circ$
 a = 75 mm b = 230 mm c = 30 mm	 103 mm $-19^\circ$	 77 mm $-17^\circ$
 a = 30 mm b = 230 mm c = 75 mm	 41 mm $32^\circ$	 102 mm $17^\circ$

TABLE I

EXPERIMENTAL RESULTS. THE SOFTFOOT DESIGN IS COMPARED TO THE RIGID FLAT FOOT IN TERMS OF LINEAR EXTENSION OF THE SUPPORT POLYGON (SUPPORT LENGTH) AND COMPENSATORY ANKLE PITCH ANGLE TO KEEP THE LEG VERTICAL (ANKLE PITCH).

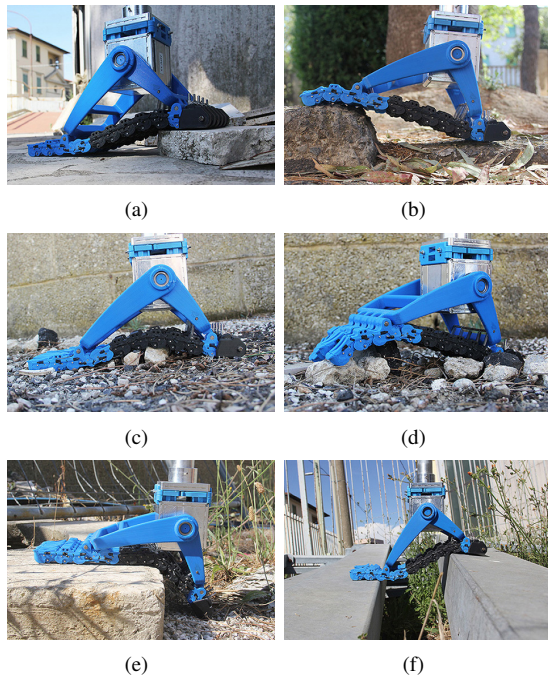


Fig. 9. The SoftFoot performing some passive adaptive poses on real uneven terrain. (a) step on flat terrain, (b) stone on a irregular ground, (c) stones under the *Planar Fascia*, (d) stones with different heights, (e) big step, and (f) crossing two beams.

## REFERENCES

- [1] Alin Albu-Schaffer, Oliver Eiberger, Markus Grebenstein, Sami Hadadin, Christian Ott, Thomas Wimbock, Sebastian Wolf, and Gerd Hirzinger. Soft robotics. *IEEE Robotics & Automation Magazine*, 15(3):20–30, 2008.
- [2] Antonio Bicchi, Marco Gabiccini, and Marco Santello. Modelling natural and artificial hands with synergies. *Philosophical Transactions of the Royal Society of London B: Biological Sciences*, 366(1581):3153–3161, 2011.
- [3] Antonio Bicchi, J Kenneth Salisbury, and David L Brock. Contact sensing from force measurements. *The International Journal of Robotics Research*, 12(3):249–262, 1993.
- [4] Lionel Birglen, Thierry Laliberté, and Clément M Gosselin. *Under-actuated robotic hands*, volume 40. Springer, 2007.
- [5] Boston dynamics website. <http://www.bostondynamics.com>. Accessed: 2016-03-01.
- [6] Branko Brackx, Michaël Van Damme, Arnout Matthys, Bram Vanderborght, and Dirk Lefeber. Passive ankle-foot prosthesis prototype with extended push-off. *Int. J. Adv. Robot. Syst.*, 2013.
- [7] Brian G Buss, Amin Ramezani, Kaveh Akbari Hamed, Brent A Griffin, Kevin S Galloway, and Jessy W Grizzle. Preliminary walking experiments with underactuated 3d bipedal robot marlo. In *Intelligent Robots and Systems (IROS 2014)*, 2014 *IEEE/RSJ International Conference on*, pages 2529–2536. IEEE, 2014.
- [8] Stéphane Caron, Quang-Cuong Pham, and Yoshihiko Nakamura. Zmp support areas for multi-contact mobility under frictional constraints. *arXiv preprint arXiv:1510.03232*, 2015.
- [9] Manuel G Catalano, Giorgio Grioli, Edoardo Farnioli, Alessandro Serio, Cristina Piazza, and Antonio Bicchi. Adaptive synergies for the design and control of the pisa/it soft hand. *The International Journal of Robotics Research*, 33(5):768–782, 2014.
- [10] Steve Davis and Darwin G Caldwell. The design of an anthropomorphic dexterous humanoid foot. In *Intelligent Robots and Systems (IROS)*, 2010 *IEEE/RSJ International Conference on*, pages 2200–2205. IEEE, 2010.
- [11] David Gouaillier, Vincent Hugel, Pierre Blazevic, Chris Kilner, Jérôme Monceaux, Pascal Lafourcade, Brice Marnier, Julien Serre, and Bruno Maisonnier. Mechatronic design of nao humanoid. In *Robotics and Automation, 2009. ICRA'09. IEEE International Conference on*, pages 769–774. IEEE, 2009.
- [12] Hugh M Herr and Alena M Grabowski. Bionic ankle-foot prosthesis normalizes walking gait for persons with leg amputation. *Proceedings of the Royal Society of London B: Biological Sciences*, 279(1728):457–464, 2012.
- [13] JH Hicks. The mechanics of the foot: Ii. the plantar aponeurosis and the arch. *Journal of anatomy*, 88(Pt 1):25, 1954.
- [14] David Hill and Hugh Herr. Effects of a powered ankle-foot prosthesis on kinetic loading of the contralateral limb: A case series. In *Rehabilitation Robotics (ICORR)*, 2013 *IEEE International Conference on*, pages 1–6. IEEE, 2013.
- [15] B.M. Hillberry and A.S. Hall Jr. Rolling contact joint, January 13 1976. US Patent 3,932,045.
- [16] Shuuji Kajita, Fumio Kanehiro, Kenji Kaneko, Kiyoshi Fujiwara, Kensuke Harada, Kazuhito Yokoi, and Hirohisa Hirukawa. Biped walking pattern generation by using preview control of zero-moment point. In *Robotics and Automation, 2003. Proceedings. ICRA'03. IEEE International Conference on*, volume 2, pages 1620–1626. IEEE, 2003.
- [17] Kenji Kaneko, Kensuke Harada, Fumio Kanehiro, Go Miyamori, and Kazuhiko Akachi. Humanoid robot hrp-3. In *Intelligent Robots and Systems, 2008. IROS 2008. IEEE/RSJ International Conference on*, pages 2471–2478. IEEE, 2008.
- [18] Hyun-jin Kang, Kenji Hashimoto, Hideki Kondo, Kentaro Hattori, Kosuke Nishikawa, Yuichiro Hama, Hun-ok Lim, Atsuo Takamishi, Keisuke Suga, and Keisuke Kato. Realization of biped walking on uneven terrain by new foot mechanism capable of detecting ground surface. In *Robotics and Automation (ICRA)*, 2010 *IEEE International Conference on*, pages 5167–5172. IEEE, 2010.
- [19] Daniel Kuehn, Frank Beinersdorf, Felix Bernhard, Kristin Fondahl, Moritz Schilling, Marc Simnonske, Tobias Stark, and Frank Kirchner. Active spine and feet with increased sensing capabilities for walking robots. In *International Symposium on Artificial Intelligence, Robotics and Automation in Space (iSAIRAS-12)*, pages 4–6, 2012.
- [20] Jianxi Li, Qiang Huang, Weimin Zhang, Zhanguo Yu, and Kejie Li. Flexible foot design for a humanoid robot. In *Automation and Logistics, 2008. ICAL 2008. IEEE International Conference on*, pages 1414–1419. IEEE, 2008.
- [21] Ahmad Najmuddin, Yoshitaka Fukuoka, and Satoshi Ochiai. Experimental development of stiffness adjustable foot sole for use by bipedal robots walking on uneven terrain. In *System Integration (SII)*, 2012 *IEEE/SICE International Symposium on*, pages 248–253. IEEE, 2012.
- [22] Francesca Negrello, Manolo Garabini, Manuel Giuseppe Catalano, P. Kryczka, W. Choi, D.G. Caldwell, A. Bicchi, and N.G. Tsagarakis. Walk-man humanoid lower body design optimization for enhanced physical performance. In *Robotics and Automation, 2016. ICRA'16. IEEE International Conference on*, 2016.
- [23] Ill-Woo Park, Jung-Yup Kim, Jungho Lee, and Jun-Ho Oh. Mechanical design of humanoid robot platform khr-3 (kaist humanoid robot 3: Hubo). In *Humanoid Robots, 2005 5th IEEE-RAS International Conference on*, pages 321–326. IEEE, 2005.
- [24] Marko B Popovic, Ambarish Goswami, and Hugh Herr. Ground reference points in legged locomotion: Definitions, biological trajectories and control implications. *The International Journal of Robotics Research*, 24(12):1013–1032, 2005.
- [25] Reinhard Putz and Reinhard Pabst. *Sobotta-Atlas of Human Anatomy: Head, Neck, Upper Limb, Thorax, Abdomen, Pelvis, Lower Limb; Two-volume set*. 2006.
- [26] Philippe Sardain and Guy Bessonnet. Forces acting on a biped robot. center of pressure-zero moment point. *IEEE Transactions on Systems, Man, and Cybernetics-Part A: Systems and Humans*, 34(5):630–637, 2004.
- [27] Tomoya Sato, Sho Sakaino, and Kouhei Ohnishi. Stability index for biped robot moving on rough terrain. *IEEE Transactions on Industry Applications*, 129(6), 2009.
- [28] Jong-Tae Seo and Byung-Ju Yi. Modeling and analysis of a biomimetic foot mechanism. In *2009 IEEE/RSJ International Conference on Intelligent Robots and Systems*, pages 1472–1477. IEEE, 2009.
- [29] Nikos G Tsagarakis, Zhibin Li, Jody Saglia, and Darwin G Caldwell. The design of the lower body of the compliant humanoid robot “ccub”. In *Robotics and Automation (ICRA)*, 2011 *IEEE International Conference on*, pages 2035–2040. IEEE, 2011.
- [30] Eric R Westervelt, Jessy W Grizzle, Christine Chevallereau, Jun Ho Choi, and Benjamin Morris. *Feedback control of dynamic bipedal robot locomotion*, volume 28. CRC press, 2007.